Physics Letters B 765 (2017) 323–327

Contents lists available at ScienceDirect

Physics Letters B

www.elsevier.com/locate/physletb

Cold and hot nuclear matter effects on charmonium production in p+Pb collisions at LHC energy

Baoyi Chen [a], Tiecheng Guo [a,b], Yunpeng Liu [a], Pengfei Zhuang [b,*]

[a] Physics Department, Tianjin University, Tianjin 300352, China
[b] Physics Department, Tsinghua University, Beijing 100084, China

ARTICLE INFO

Article history:
Received 1 August 2016
Received in revised form 29 November 2016
Accepted 8 December 2016
Available online 12 December 2016
Editor: W. Haxton

Keywords:
Quarkonium production
Heavy ion collisions
Cold medium effect
Hot medium effect

ABSTRACT

We study cold and hot nuclear matter effects on charmonium production in p+Pb collisions at $\sqrt{s_{\rm NN}} = 5.02$ TeV in a transport approach. At the forward rapidity, the cold medium effect on all the $c\bar{c}$ states and the hot medium effect on the excited $c\bar{c}$ states only can explain well the J/ψ and ψ' yield and transverse momentum distribution measured by the ALICE collaboration, and we predict a significantly larger ψ' $p_{\rm T}$ broadening in comparison with J/ψ. However, we can not reproduce the J/ψ and ψ' data at the backward rapidity with reasonable cold and hot medium effects.

There are two kinds of nuclear matter effects on charmonium production in heavy ion collisions [1]. One is the hot nuclear matter effect during the evolution of the fireball, and the other is the cold nuclear matter effect before the formation of the fireball. The former includes color screening [2] and regeneration [3–6] which work in an opposite way and lead respectively to charmonium suppression and enhancement. The later contains mainly the shadowing effect [7–10], Cronin effect [11,12] and nuclear absorption [13]. Different from nucleus–nucleus (A+B) collisions where both cold and hot medium effects are important and charmonia are considered as a sensitive probe of the Quark-Gluon Plasma (QGP) formation, for proton–nucleus (p+A) collisions it is expected that, there might be no fireball during the evolution of the system and the cold medium controls the charmonium production. Small systems are theoretically investigated in many approaches like energy loss model [14], transport model [15] and comover model [16].

Recently, the ALICE collaboration measured the nuclear modification factor $R_{\rm pA}$ and averaged transverse momentum square $\langle p_{\rm T}^2\rangle_{\rm pA}$ for J/ψ and ψ' in p+Pb collisions at $\sqrt{s_{NN}} = 5.02$ TeV [17–20]. In particular the new data display two interesting features at forward rapidity: a much stronger ψ' suppression than J/ψ (see Fig. 2) and an increasing $p_{\rm T}$ broadening with centrality (see Fig. 3). At LHC energy, the collision time is much shorter than the charmonium formation time and the QGP formation time, and the cold medium effect on the ground and excited states of $c\bar{c}$ are almost the same. Therefore, the difference between J/ψ and ψ' suppression shown in Fig. 2 tells us that there should be a hot medium effect which is strong for ψ' but weak for J/ψ. Since the regenerated charmonia in the fireball carry lower momentum in comparison with the initially produced charmonia, a sizeable regeneration will break down the linear increase of $\langle p_{\rm T}^2\rangle$ [21,22] shown in Fig. 3. Taking into account these two hints extracted from the data, we will consider in this paper the hot medium effect only on the excited state and neglect the regeneration in p+A collisions.

Generally, the initially produced charmonium distribution f_Ψ for $\Psi = J/\psi,\ \psi',\ \chi_c$ in transverse plane in a p+A collision at fixed impact parameter $\mathbf{b}$ can be obtained through a superposition of effective nucleon–nucleon (p+p) collisions [22],

$$f_\Psi(\mathbf{p},\mathbf{x}|\mathbf{b}) = (2\pi)^3\delta(z)\delta(\mathbf{x}_{\rm T}-\mathbf{b})\int dz_{\rm A}\rho_{\rm A}(\mathbf{x}_T,z_{\rm A})\mathcal{R}(x,\mu_{\rm F},\mathbf{x}_{\rm T}) \times \frac{d\overline{\sigma}_\Psi^{\rm pp}(\mathbf{p},\mathbf{x}_{\rm T},z_{\rm A})}{d^3\mathbf{p}}, \quad (1)$$

where $\mathbf{x}_{\rm T}$ is the charmonium transverse coordinate, and $\rho_{\rm A}$ is the nucleon distribution function in nucleus A. For the two initial partons participating in the hard process of charmonium production, one is from the incident proton and the other comes from the nucleon with longitudinal coordinate $z_{\rm A}$ in nucleus A. The nuclear

* Corresponding author.
E-mail address: zhuangpf@mail.tsinghua.edu.cn (P. Zhuang).

http://dx.doi.org/10.1016/j.physletb.2016.12.021

shadowing effect is embedded in the inhomogeneous modification factor $\mathcal{R}$ [8] for the parton with longitudinal momentum fraction $x = 2m_T/\sqrt{s_{NN}}\, e^{-y}$ and factorization factor $\mu_F = m_T$ [7], where $m_T = \sqrt{m_\Psi^2 + \mathbf{p}_T^2}$ and $y = 1/2\ln((E+p_z)/(E-p_z))$ are the charmonium transverse mass and longitudinal momentum rapidity. Note that, we have assumed here that the emitted parton is soft in comparison with the initial partons and the produced charmonium and can be neglected in kinematics. Under this approximation, the charmonium production becomes a $2 \to 1$ process. We employ the model EPS09s NLO [23] to parameterize the inhomogeneous shadowing effect in our numerical calculation.

The effective cross section $\overline{\sigma}_\Psi^{pp}$ includes the Cronin effect which broadens the charmonium momentum distribution. Before the parton from nucleus A participates the hard process, it acquires additional transverse momentum via multiple scattering with the surrounded nucleons, and this extra momentum is inherited by the produced charmonium. Inspired from a random-walk picture, we take a Gaussian smearing [24,25] for the modified transverse momentum distribution

$$\overline{f}_\Psi^{pp}(\mathbf{p}, \mathbf{x}_T, z_A) = \frac{1}{\pi a_{gN} l} \int d^2\mathbf{q}_T e^{\frac{-\mathbf{q}_T^2}{a_{gN} l}} f_\Psi^{pp}(|\mathbf{p}_T - \mathbf{q}_T|, p_z), \tag{2}$$

where $l(\mathbf{x}_T, z_A)$ is the averaged moving length of the parton coming from z_A in the nucleus before its hard interaction at $\mathbf{x}_T$, a_{gN} is the averaged charmonium transverse momentum square inherited from the parton scattering with a unit length of nucleons per fm, and $f_\Psi^{pp}(\mathbf{p})$ is the momentum distribution for a free p+p collision. The length l is calculated from the nuclear geometry, and the value of the Cronin parameter is extracted as $a_{gN} = 0.15$ GeV^2/fm by fitting the data in $\sqrt{s_{NN}} = 2.76$ TeV Pb–Pb collisions [25]. We take the same value at $\sqrt{s_{NN}} = 5.02$ TeV.

Currently there is no experimental distribution f_Ψ^{pp} for free p+p collisions at $\sqrt{s_{NN}} = 5.02$ TeV. We take the same parameterization formula [22] used to fit the experimental data at $\sqrt{s_{NN}} =$ 200 GeV [26], 2.76 TeV [27] and 7 TeV [28],

$$\frac{d^2\sigma_\Psi^{pp}}{dy p_T dp_T} = \frac{d\sigma_\Psi^{pp}}{dy} \frac{(n-1)}{\pi(n-2)\langle p_T^2\rangle_\Psi^{pp}} \left(1 + \frac{p_T^2}{(n-2)\langle p_T^2\rangle_\Psi^{pp}}\right)^{-n}, \tag{3}$$

where $d\sigma_\Psi^{pp}/dy = d\sigma_\Psi^{pp}/dy|_{y=0} e^{-0.06418y^2}$ and $\langle p_T^2\rangle_\Psi^{pp}(y) = \langle p_T^2\rangle_\Psi^{pp}(0)\left(1 - (y/y_{max})^2\right)$ are the rapidity dependence of the production cross section and averaged transverse momentum square. By linearly fitting their central values with the data at $\sqrt{s_{NN}} =$ 2.76 TeV and 7 TeV, we obtain $d\sigma_\Psi^{pp}/dy|_{y=0} = 5.01$ μb and $\langle p_T^2\rangle_\Psi^{pp}(0) = 12.5$ (GeV/c)^2 at $\sqrt{s_{NN}} = 5.02$ TeV. Then by fitting the normalized p_T distribution with PYTHIA [29], we choose the parameter $n = 3.2$. Note that we have here neglected the energy dependence of the width of the cross section $d\sigma_\Psi^{pp}/dy$ from 2.76 TeV to 5.02 TeV. The parameterization used here is similar to the one in the energy loss model [14] for the calculation of J/ψ and Υ suppression at LHC energy.

With the phase-space distribution (1) as the initial condition at time τ_0 when the fireball is formed, the evolution of the initially produced charmonia in the hot medium can be described in a transport approach [6,30]. Neglecting the regeneration in p+A collisions mentioned above, the charmonia satisfy the transport equation [31]

$$\left[\cosh(y-\eta)\frac{\partial}{\partial\tau} + \frac{\sinh(y-\eta)}{\tau}\frac{\partial}{\partial\eta} + \mathbf{v}_T\cdot\nabla_T\right] f_\Psi = -\alpha_\Psi f_\Psi \tag{4}$$

where $\mathbf{v}_T = \mathbf{p}_T/E_T$ and $\eta = 1/2\ln((t+z)/(t-z))$ are respectively the charmonium transverse velocity and longitudinal coordinate rapidity. The second and third terms on the left hand side represent the leakage effect on charmonium motion in the longitudinal direction and transverse plane. The charmonia with large velocity can escape from the hot medium by free streaming. This effect will increase the charmonium transverse momentum in nuclear collisions [30]. The charmonium suppression in the hot medium is reflected in the loss term α_Ψ [6],

$$\alpha_\Psi(\mathbf{p}, \mathbf{x}, t, T) = \frac{1}{2E_T}\int \frac{d^3\mathbf{k}}{(2\pi)^3 2E_g} F_{g\Psi}(\mathbf{p}, \mathbf{k})\sigma_{g\Psi}(\mathbf{p}, \mathbf{k}, T) f_g(\mathbf{k}, T), \tag{5}$$

where we have considered the gluon dissociation $g + \Psi \to c + \bar{c}$ as the dominant dissociation process in the hot QGP, and E_g and $\mathbf{k}$ are the gluon energy and momentum. The cross section $\sigma_{g\Psi}$ in vacuum can be derived through the operator production expansion with perturbative Coulomb wave function [32,33], and its temperature dependence can be obtained by taking into account the geometrical relation between the cross section and the average size of the charmonium state, $\sigma_{g\Psi}(T) = \sigma_{g\Psi}(0)\langle r_\Psi^2\rangle(T)/\langle r_\Psi^2\rangle(0)$. The averaged radius squared $\langle r_\Psi^2\rangle$ can be calculated from the potential model [34], its divergence self-consistently defines a Mott dissociation temperature T_d^Ψ which indicates the melting of the bound state due to color screening. In this sense, the cross section in medium can also be approximately written as $\sigma_{g\Psi}(T) = \sigma_{g\Psi}(0)/\Theta(T_d^\Psi - T)$.

The thermal gluon distribution $f_g = 16/(e^{k_\mu u^\mu/T} - 1)$ in (5) is controlled by the local temperature $T(\mathbf{x}, t)$ and fluid velocity $u_\mu(\mathbf{x}, t)$ which are determined by the hydrodynamics of the hot medium,

$$\partial_\mu T^{\mu\nu} = 0 \tag{6}$$

with the energy–momentum tensor $T^{\mu\nu}$. In order to close the hydrodynamic equations, one needs the equation of state of the medium. We follow Ref. [35] where the deconfined phase at high temperature is an ideal gas of gluons and massless u and d quarks plus 150 MeV mass s quarks, and the hadron phase at low temperature is an ideal gas of all known hadrons and resonances with mass up to 2 GeV [36]. There is a first-order phase transition between these two phases with the critical temperature $T_c = 165$ MeV at vanishing baryon density.

We choose the initial time of the hot medium to be $\tau_0 = 0.6$ fm [37] and determine the spatial dependence of the initial energy density of the medium by the Glauber model. Taking into account the hint from the analysis of the data that the hot medium affects only the excited charmonium states, the fireball temperature is in between the ψ' and J/ψ dissociation temperatures $T_d^{\psi'} \simeq T_c$ and $T_d^{J/\psi} \simeq 1.5T_c$. To be specific, we choose in the following numerical calculation the maximum temperature at the center of the fireball to be $T_0 = 180$ MeV. The profile of the initial temperature in central p+Pb collisions at $\sqrt{s_{NN}} = 5.02$ TeV is shown in Fig. 1. In this case the initial hot medium is in the QGP phase with fireball radius $r < 0.8$ fm and enters the mixed phase at 0.8 fm $< r <$ 1.1 fm where the QGP fraction changes from 1 to 0. The temperature jumps down rapidly afterwards. From our numerical calculation, the obtained charmonium distributions R_{pA} and $\langle p_T^2\rangle$ shown in the following are not sensitive to the value of T_0 when it satisfies the constraint $T_d^{\psi'} < T_0 < T_d^{J/\psi}$.

The inclusive charmonia measured by the ALICE Collaboration include the prompt part and the contribution from B-hadron decay [38–40]. The former consists of direct production and feed-down from the excited states, 30% from χ_c and 10% from ψ', and the latter comes from the decay of bottom hadrons. Since the ALICE experiment does not separate the two parts from each

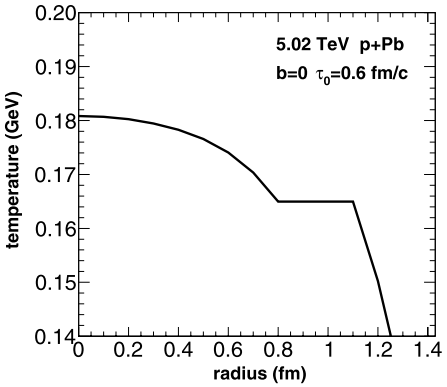

Fig. 1. The initial temperature distribution as a function of the fireball radius in central p+Pb collisions at colliding energy $\sqrt{s_{\rm NN}} = 5.02$ TeV.

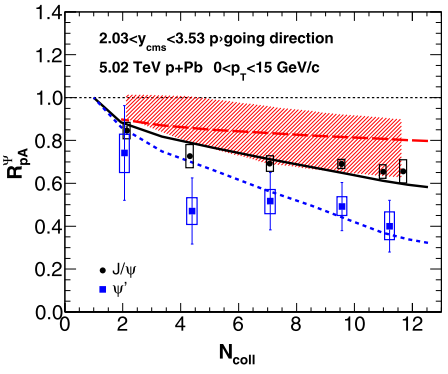

Fig. 2. (Color online.) The nuclear modification factor $R^{\Psi}_{\rm pA}(N_{\rm coll})$ in p+Pb collisions at forward rapidity. The dashed line shows the result with only nuclear shadowing (EPS09s NLO [23]) and the band indicates the uncertainty [20]. The solid and dotted lines are respectively the full calculations for inclusive J/ψ and ψ', and the data are from the ALICE Collaboration [20,42].

other, we have to take into account the B decay contribution to compare our model calculation with the ALICE data. From the inclusive J/ψ data in p+p collisions, the transverse momentum dependence of the B decay fraction can be well parameterized as $f_{\rm B\to\Psi} = f_0 + kp_{\rm T}$ with $f_0 = 0.04$ and $k = 0.023$ c/GeV for J/ψ [41] and $f_0 = 0.114$ and $k = 0.0217$ c/GeV for ψ' [38]. The linear parametrization is rapidity independent in the region we considered and the parameters f_0 and k are also colliding energy independent for 2 TeV $< \sqrt{s_{\rm NN}} <$ 7 TeV [41].

Including the contributions from the direct production controlled by the transport equation (4) and the decay from excited states and B hadrons, we now calculate the charmonium distributions in the final state and compare them with the ALICE data. We start with the charmonium nuclear modification factor $R^{\Psi}_{\rm pA} = N^{\Psi}_{\rm pA}/(N_{\rm coll}N^{\Psi}_{\rm pp})$, where $N_{\rm coll}$ is the number of binary collisions which can be calculated from the nuclear geometry at fixed centrality, and $N^{\Psi}_{\rm pp}$ and $N^{\Psi}_{\rm pA}$ are respectively the numbers of charmonia measured in p+p and p+A collisions. Our calculated $R_{\rm pA}$ as a function of $N_{\rm coll}$ for J/ψ and ψ' and the comparison with the inclusive ALICE data for p+Pb collisions at $\sqrt{s_{\rm NN}} = 5.02$ TeV are shown in Fig. 2 at forward rapidity.

The nuclear shadowing is reflected in the initial condition (1) of the transport equation (4). To account for the spatial dependence of the shadowing in a finite nucleus, we take EPS09s NLO [23] to parameterize the inhomogeneous modification factor $\mathcal{R}$ where the charmonium position dependence is embedded through the nuclear geometry. As is well known, the shadowing effect on charmonium production in nuclear collisions depends strongly on the charmonium rapidity y. From the relation between the parton momentum fraction and the charmonium rapidity $x \sim e^{-y}$, there is a strong shadowing at forward rapidity and antishadowing at backward rapidity in nuclear collisions at LHC energy. This provides a chance to see clearly the cold nuclear matter effect on charmonium distributions in different rapidity bins. The shadowing effect leads already to a sizeable charmonium suppression at the forward rapidity, see the dashed line in Fig. 2. The band is the result with uncertainty in the shadowing [20]. Note that the cold medium effect at LHC energy is the same for the ground and excited $c\bar{c}$ states. While the maximum shadowing effect (the lower limit of the band) can reasonably explain the J/ψ data, the much more strong ψ' suppression needs a significant hot medium effect. Taking the initial fireball temperature shown in Fig. 1, we can explain the J/ψ and ψ' yield reasonably well, see the solid and dotted lines in Fig. 2. The results can be understood through the following analysis. Since the cold and hot nuclear matter effects happen in different time regions, they independently affect the charmonium production. Introducing the cold and hot medium induced modification factors $R^{\rm cold}_{\rm pA}$ and $R^{\rm hot}_{\rm pA}$ and considering the fact that 40% of the finally measured J/ψs come from the decay of the excited states ψ' and χ_c, $R^{\Psi}_{\rm pA}$ can be expressed as

$$R^{\psi'}_{\rm pA} = R^{\rm cold}_{\rm pA} R^{\rm hot}_{\rm pA},$$
$$R^{J/\psi}_{\rm pA} = 0.6R^{\rm cold}_{\rm pA} + 0.4R^{\psi'}_{\rm pA}. \quad (7)$$

For very central collisions where the cold and hot medium effects are the strongest, taking $R^{\rm cold}_{\rm pA} = 0.8$ from the EPS09s NLO parametrization shown in Fig. 2 and $R^{\rm hot}_{\rm pA} = 0.5$ lead to $R^{\psi'}_{\rm pA} = 0.4$ and $R^{J/\psi}_{\rm pA} = 0.64$. For semi-central collisions with $N_{\rm coll} = 6$ where the cold and hot medium effects become weaker, taking $R^{\rm cold}_{\rm pA} = 0.85$ and $R^{\rm hot}_{\rm pA} = 0.7$ result in $R^{\psi'}_{\rm pA} = 0.6$ and $R^{J/\psi}_{\rm pA} = 0.75$.

The $R_{\rm pA}(N_{\rm coll})$ as a function of centrality is a global quantity, the momentum integration smears the fireball structure and the cold and hot nuclear matter effects. To have a deep insight into what is happening to the quarkonium motion in the hot medium, one needs to concentrate on the quarkonium momentum distribution. Different from the longitudinal motion which inherits the initial colliding kinematics via momentum conservation, the transverse motion in heavy ion collisions is developed during the dynamical evolution of the system. The microscopically high particle density and multiple scatterings play an essential role in the development of the finally observed transverse momentum distribution. The distribution is therefore sensitive to the medium properties, such as the equation of state. For quarkonia, we expect that their transverse momentum distribution can help us to probe the detailed structure of the fireball and differentiate between the production and suppression mechanisms.

We now turn to the calculation of the averaged transverse momentum square where the Cronin effect plays an important role. The difference $\langle p^2_{\rm T}\rangle_{\rm pA} - \langle p^2_{\rm T}\rangle_{\rm pp}$ between the p+Pb and p+p collisions is shown in Fig. 3 as a function of $N_{\rm coll}$. By the definition, the difference should disappear at $N_{coll} = 2$. However, it is not zero from the experimental measurement, due to the lack of the p+p data at $\sqrt{s_{\rm NN}} = 5.02$ TeV, see the explanation by the ALICE collaboration [20]. In this case, we take the experiment measured difference at $N_{coll} = 2$ as the input in our model calculation. With the initial charmonium distribution (1) including shadowing and Cronin effects, the cold medium induced momentum difference is shown as the dashed line in Fig. 3. While there is a weak $p_{\rm T}$ dependence of the nuclear shadowing (it becomes stronger at low $p_{\rm T}$ [19]), the linear increase of the momentum difference comes mainly from the Cronin effect described by equation (2).

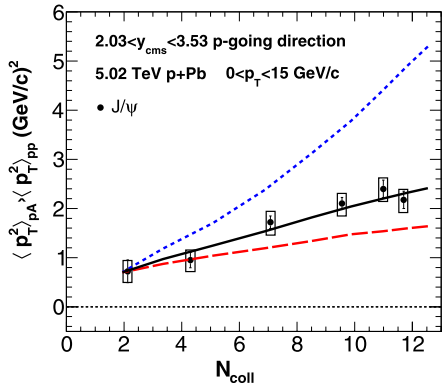

Fig. 3. (Color online.) The medium induced momentum change $\langle p_T^2\rangle_{pA} - \langle p_T^2\rangle_{pp}$ in p+Pb collisions at forward rapidity. The dashed line shows the result with only cold nuclear matter effect, and the solid and dotted lines are respectively the full calculations for inclusive J/ψ and ψ'. The data for J/ψ are from the ALICE Collaboration [20].

Note that the dashed line is for any $c\bar{c}$ state and does not distinguish between J/ψ and ψ'. When the hot medium with temperature $T_d^{\psi'} < T < T_d^{J/\psi}$ is turned on, the directly produced J/ψs are not affected, but ψ's are extremely suppressed due to the leakage effect: the fast moving ψ's escape from the QGP phase but the slow ψ's are eaten up by the hot medium. This leads to a strong p_T broadening for ψ's, especially in central collisions where the leakage is most important, see the dotted line in Fig. 3. Considering the fact that 40% of the finally measured J/ψs are from the decay of the excited states, the leakage induced ψ' p_T broadening enhances also the J/ψ transverse momentum sizeably, see the solid line in Fig. 3. The strong enhancement of averaged transverse momentum square for ψ' can be considered as a signal of the hot medium effect in p+Pb collisions and it needs to be experimentally confirmed.

The differential nuclear modification factor $R_{pA}(p_T)$ as a function of transverse momentum is shown in Fig. 4 for inclusive J/ψ and ψ' in minimum bias (corresponding to an average impact parameter b=5 fm from a Glauber calculation) p+Pb collisions at $\sqrt{s_{NN}} = 5.02$ TeV at forward rapidity. The band is the result including only nuclear shadowing parameterized by EPS09s NLO [23]. It clearly deviates from the data, especially the data for ψ'. The full calculations with both cold and hot nuclear matter effects are shown as solid and dotted lines for J/ψ and ψ', they roughly agree with the data. The increasing R_{pA} with p_T indicates the strong suppression at low p_T and weak suppression at high p_T induced by the leakage effect discussed above. The almost p_T independent difference between J/ψ and ψ' shows that, there is no suppression for direct J/ψ and only the excited states are affected by the hot medium.

We now extend our calculation to the backward rapidity. The momentum integrated nuclear modification factor R_{pA} as a function of N_{coll} is shown in Fig. 5. The big difference between the two rapidity regions is the shadowing at forward rapidity and antishadowing at backward rapidity. This can be seen clearly in Figs. 2 and 5 where the cold medium induced modification R_{pA} (dashed lines) is below unity at forward rapidity but above unity at backward rapidity. Taking the same hot medium as at the forward rapidity, while the calculated modification factor $R_{pA}^{\psi'}$ at the backward rapidity agrees roughly with the data, the calculation for J/ψ is opposite to the data: J/ψ is suppressed in the calculation but in data it is enhanced and the enhancement increases with centrality. Is it possible to reproduce the J/ψ and ψ' data with reasonable cold and hot medium effects? The answer is negative. From Fig. 5

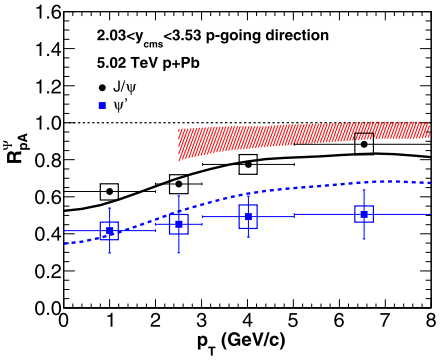

Fig. 4. (Color online.) The nuclear modification factor $R_{pA}^{\Psi}(p_T)$ in minimum bias p+Pb collisions at forward rapidity. The band is the result with only nuclear shadowing (EPS09s NLO [23]). The solid and dotted lines are respectively the full calculations for inclusive J/ψ and ψ', and the data are from the ALICE Collaboration [18].

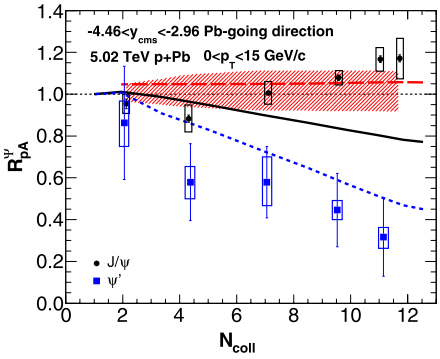

Fig. 5. (Color online.) The nuclear modification factor $R_{pA}^{\Psi}(N_{coll})$ in p+Pb collisions at backward rapidity. The dashed line shows the result with only nuclear shadowing (EPS09s NLO [23]) and the band indicates the uncertainty. The solid and dotted lines are respectively the full calculations for inclusive J/ψ and ψ', and the data are from the ALICE Collaboration [20,42].

and Eq. (7), to fit $R_{pA}^{\psi'} = 0.3$ and $R_{pA}^{J/\psi} = 1.1$ in central collisions, one has to have $R_{pA}^{cold} = 1.63$ and $R_{pA}^{hot} = 0.18$. The cold medium effect is too strong and far beyond the upper limit of the normally parameterized antishadowing [7,43]. The hot medium effect is also extremely strong and far beyond the expectation for p+A collisions (remember $R_{pA}^{hot} = 0.5$ at forward rapidity). The differential nuclear modification factor $R_{pA}(p_T)$ in minimum bias (impact parameter b=5 fm) p+Pb collisions at backward rapidity is shown in Fig. 6. The band is the result including only nuclear shadowing parameterized by EPS09s NLO [23]. Again the calculation for ψ' with both cold and hot nuclear matter effects can roughly reproduce the data. For J/ψ, the data show enhancement at any p_T, but the model shows a strong suppression at low p_T. There seems no way to remove this big difference by cold and hot medium effects. The p_T integrated nuclear modification factor at forward and backward rapidity in minimum bias (impact parameter b=5 fm) p+Pb collisions is shown in Fig. 7. At forward rapidity the cold and hot medium effects together can explain the data within error bars. At backward rapidity, however, while the ψ' suppression can be reproduced through the strong leakage effect, the J/ψ enhancement is beyond the scope of the medium effects.

In above calculations we did not consider the hot medium effect at hadron level which may play a role in p+A collisions [16]. However, the puzzle of J/ψ enhancement at backward rapidity shown in Figs. 5–7 is still hard to be solved by including hadron matter. If the QGP phase is followed by a hadron phase, the extra hot medium effect leads to an extra charmonium suppression which will enhance the difference between the theory and

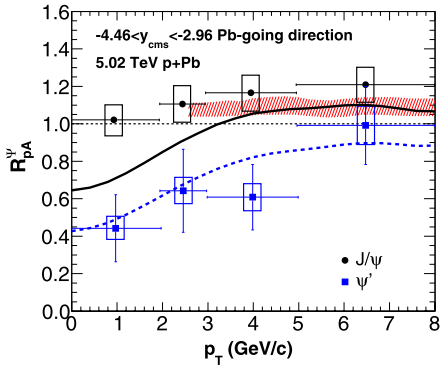

Fig. 6. (Color online.) The nuclear modification factor $R^{\Psi}_{\rm pA}(p_{\rm T})$ in minimum bias p+Pb collisions at backward rapidity. The band is the result with only nuclear shadowing (EPS09s NLO [23]). The solid and dotted lines are respectively the full calculations for inclusive J/ψ and ψ', and the data are from the ALICE Collaboration [18].

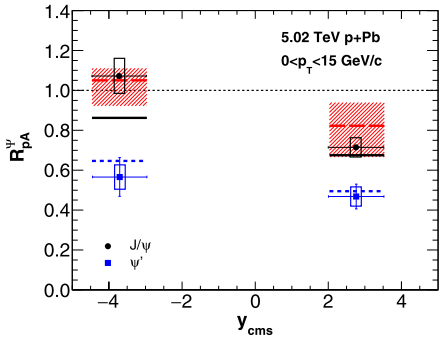

Fig. 7. (Color online.) The $p_{\rm T}$-integrated nuclear modification factor $R^{\Psi}_{\rm pA}$ at forward and backward rapidity in minimum bias p+Pb collisions. The dashed lines show the result with only nuclear shadowing (EPS09s NLO [23]) and the bands indicate the uncertainty. The solid and dotted lines are respectively the full calculations for inclusive J/ψ and ψ', and the data are from the ALICE Collaboration [18].

the data. If the system experiences only a hadron phase, the hot medium effect together with the antishadowing $R^{\rm cold}_{\rm pA} = 1.2$ described by EPS09 LO leads to a J/ψ suppression with $R^{J/\psi}_{\rm pA} = 0.95$ [16] at the backward rapidity. When we take EPS09 NLO with $R^{\rm cold}_{\rm pA} = 1.05$ shown in Fig. 5 to replace EPS09 LO, there is $R^{J/\psi}_{\rm pA} = 0.8$ in the hadron model which is consistent with our result shown in Fig. 5.

In summary, we investigated charmonium production in p+Pb collisions at colliding energy $\sqrt{s_{\rm NN}} = 5.02$ TeV. The cold nuclear matter effect on all $c\bar{c}$ states and hot nuclear matter effect on the excited $c\bar{c}$ states only can explain well the charmonium yield and transverse momentum distribution at forward rapidity. In comparison with J/ψ, the hot medium effect leads to a significant $p_{\rm T}$ broadening for ψ'. However, we can not simultaneously reproduce the charmonium $R_{\rm pA}$ and $\langle p^2_{\rm T}\rangle_{\rm pA}$ at backward rapidity with reasonable cold and hot medium effects. There seems to be something new at the backward rapidity.

Acknowledgements

The work is supported by the NSFC and MOST grant Nos. 11335005, 11575093, 11547043, 2013CB922000, 2014CB845400 and Tsinghua University Initiative Scientific Research Program.

References

[1] A. Andronic, et al., Eur. Phys. J. C 76 (2016) 107.
[2] T. Matsui, H. Satz, Phys. Lett. B 178 (1986) 416.
[3] P. Braun-Munzinger, J. Stachel, Phys. Lett. B 490 (2000) 196; A. Andronic, P. Braun-Munzinger, K. Redlich, J. Stachel, Phys. Lett. B 571 (2003) 36.
[4] R.L. Thews, M. Schroedter, J. Rafelski, Phys. Rev. C 63 (2001) 054905.
[5] L. Grandchamp, R. Rapp, Phys. Lett. B 523 (2001) 60.
[6] L. Yan, P. Zhuang, N. Xu, Phys. Rev. Lett. 97 (2006) 232301.
[7] K.J. Eskola, V.J. Kolhinen, C.A. Salgado, Eur. Phys. J. C 9 (1999) 61.
[8] R. Vogt, Phys. Rev. C 71 (2005) 054902.
[9] D. de Florian, R. Sassot, Phys. Rev. D 69 (2004) 074028.
[10] K.J. Eskola, H. Paukkunen, C.A. Salgado, J. High Energy Phys. 0807 (2008) 102.
[11] J.W. Cronin, et al., Phys. Rev. D 11 (1975) 3105.
[12] S. Gavin, M. Gyulassy, Phys. Lett. B 214 (1988) 241.
[13] C. Gerschel, J. Hüfner, Phys. Lett. B 207 (1988) 253.
[14] F. Arleo, R. Kolevatov, S. Peigné, M. Rustamova, J. High Energy Phys. 1305 (2013) 155.
[15] X. Du, R. Rapp, Nucl. Phys. A 943 (2015) 147.
[16] E.G. Ferreiro, Phys. Lett. B 749 (2015) 98.
[17] B.B. Abelev, et al., ALICE Collaboration, J. High Energy Phys. 1402 (2014) 073.
[18] B.B. Abelev, et al., ALICE Collaboration, J. High Energy Phys. 1412 (2014) 073.
[19] J. Adam, et al., ALICE Collaboration, J. High Energy Phys. 1506 (2015) 055.
[20] J. Adam, et al., ALICE Collaboration, J. High Energy Phys. 1511 (2015) 127.
[21] K. Zhou, N. Xu, P. Zhuang, Nucl. Phys. A 834 (2010) 249C.
[22] K. Zhou, N. Xu, Z. Xu, P. Zhuang, Phys. Rev. C 89 (2014) 054911.
[23] I. Helenius, K.J. Eskola, H. Honkanen, C.A. Salgado, J. High Energy Phys. 1207 (2012) 073.
[24] X. Zhao, R. Rapp, Phys. Lett. B 664 (2008) 253.
[25] B. Chen, Phys. Rev. C 93 (2016) 054905.
[26] A. Adare, et al., PHENIX Collaboration, Phys. Rev. Lett. 98 (2007) 232002.
[27] B. Abelev, et al., ALICE Collaboration, Phys. Lett. B 718 (2012) 295.
[28] K. Aamodt, et al., ALICE Collaboration, Phys. Lett. B 704 (2011) 442, Phys. Lett. B 718 (2012) 692 (Erratum).
[29] T. Sjostrand, S. Mrenna, P.Z. Skands, J. High Energy Phys. 0605 (2006) 026.
[30] X. Zhu, P. Zhuang, N. Xu, Phys. Lett. B 607 (2005) 107.
[31] Y. Liu, Z. Qu, N. Xu, P. Zhuang, J. Phys. G 37 (2010) 075110.
[32] M.E. Peskin, Nucl. Phys. B 156 (1979) 365.
[33] G. Bhanot, M.E. Peskin, Nucl. Phys. B 156 (1979) 391.
[34] H. Satz, J. Phys. G 32 (2006) R25.
[35] J. Sollfrank, P. Huovinen, M. Kataja, P.V. Ruuskanen, M. Prakash, R. Venugopalan, Phys. Rev. C 55 (1997) 392.
[36] K. Hagiwara, et al., PDG Collaboration, Phys. Rev. D 66 (2002) 010001.
[37] Y. Liu, C.M. Ko, T. Song, Phys. Lett. B 728 (2014) 437.
[38] T. Aaltonen, et al., CDF Collaboration, Phys. Rev. D 80 (2009) 031103.
[39] S. Chatrchyan, et al., CMS Collaboration, J. High Energy Phys. 1205 (2012) 063.
[40] B. Chen, Y. Liu, K. Zhou, P. Zhuang, Phys. Lett. B 726 (2013) 725.
[41] V. Khachatryan, et al., CMS Collaboration, Eur. Phys. J. C 71 (2011) 1575.
[42] M. Leoncino, ALICE Collaboration, Nucl. Phys. A 956 (2016) 689.
[43] R. Vogt, Phys. Rev. C 81 (2010) 044903.